

SOAF: Scene Occlusion-aware Neural Acoustic Field

Huiyu Gao^{1*}, Jiahao Ma^{1,2*}, David Ahmedt-Aristizabal², Chuong Nguyen², Miaomiao Liu¹

¹Australian National University, ²CSIRO Data61

{huiyu.gao, jiahao.ma, miaomiao.liu}@anu.edu.au

{jiahao.ma, david.ahmedtaristizabal, chuong.nguyen}@data61.csiro.au

Abstract

This paper tackles the problem of novel view audio-visual synthesis along an arbitrary trajectory in an indoor scene, given the audio-video recordings from other known trajectories of the scene. Existing methods often overlook the effect of room geometry, particularly wall occlusion to sound propagation, making them less accurate in multi-room environments. In this work, we propose a new approach called Scene Occlusion-aware Acoustic Field (SOAF) for accurate sound generation. Our approach derives a prior for sound energy field using distance-aware parametric sound-propagation modelling and then transforms it based on scene transmittance learned from the input video. We extract features from the local acoustic field centred around the receiver using a Fibonacci Sphere to generate binaural audio for novel views with a direction-aware attention mechanism. Extensive experiments on the real dataset *RWAVS* and the synthetic dataset *SoundSpaces* demonstrate that our method outperforms previous state-of-the-art techniques in audio generation. Project page: <https://huiyu-gao.github.io/SOAF/>.

1 Introduction

We live in a world with rich audio-visual multi-modal information. Audio-visual scene synthesis enables the generation of videos and corresponding audio along arbitrary novel camera trajectories based on a source video with its associated audio. This task involves reconstructing the audio-visual scene both visually and acoustically from recorded real-world source videos with binaural audio along known camera trajectories. Specifically, it entails synthesising the images a person would see and the sounds that a person would hear while navigating within the scene from any novel position and direction along an arbitrary camera trajectory.

Neural Radiance Fields (NeRF) [3] has made significant progress in the field of computer vision over the past few years. NeRF uses Multi-Layer Perceptrons (MLP) to learn an implicit and continuous representation of the visual scene and synthesise novel view images through volume rendering. While NeRF has been extensively explored in the field [4–9], these methods focus solely on the visual aspect of the input video, ignoring the accompanying audio track. However, the world we live in contains multi-modal information. Most videos we capture include not only visual images but also sound signals. Therefore, investigating novel view acoustic synthesis is crucial to providing more immersive experiences for users in various AV/VR applications.

Recently, Neural Acoustic Field (NAF) [1] became the first work to explore the application of implicit representation in sound field encoding. Similar to NeRF, NAF uses an MLP to learn a continuous function of the neural acoustic field, optimising it by supervising the generated Room Impulse Response (RIR) in the time-frequency domain at different emitter-listener location pairs and view directions. For the audio-visual scene synthesis task, AV-NeRF [2] is the first multi-modal approach to address this problem. They utilise the vanilla NeRF [3] for novel view synthesis and integrate

*Equal contribution.

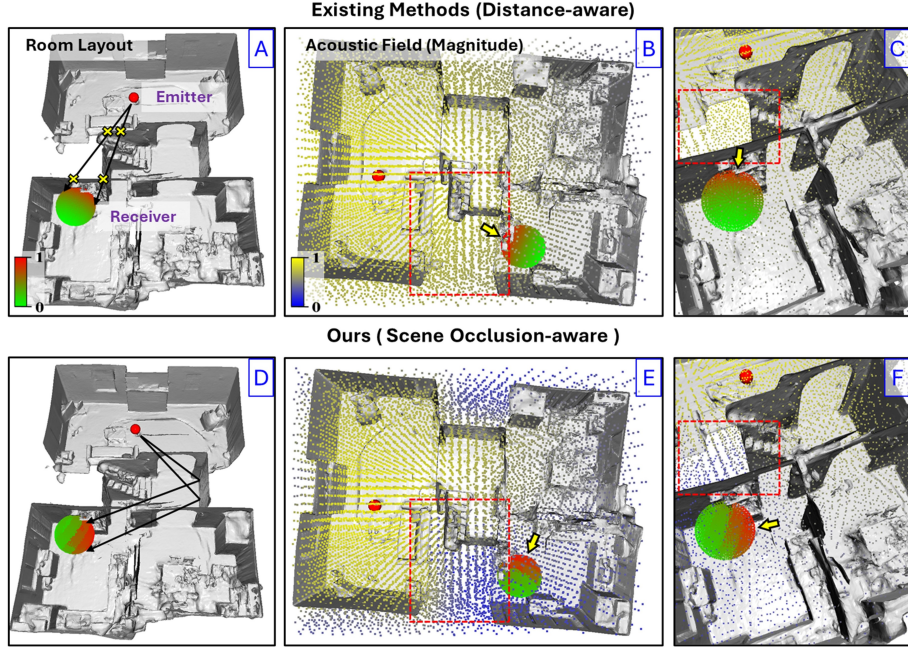


Figure 1: Pure distance-aware acoustic field [1, 2] vs. our proposed Scene Occlusion-aware Acoustic Field (SOAF). **Left column** (A & D) shows sound propagation in a room: the small ball represents the emitter and the large red-green ball represents the receiver. Coded colours indicate sound intensity, with red denoting high intensity and green denoting low intensity. **Middle column** (B & E) visualises the magnitude distribution of the acoustic field: yellow indicates high intensity and blue indicates low intensity. The comparison of sound attenuation through walls, highlighted by red dashed bounding boxes in sub-figures B, C, E and F emphasises our consideration of wall obstruction. **Right column** (C & F) highlights the existing methods’ neglects of obstruction in sound propagation in C while the proposed method in F gives higher sound intensity near the door than near the wall. Yellow crosses in A and the receiver’s sound intensity distribution in C further illustrate this point.

the rendered novel view image and depth map as visual and geometric cues into audio generation. While AV-NeRF [2] has demonstrated promising results using multi-modal data, it only renders a single image and depth map for the novel view, providing limited visual and geometric information about the scene. Moreover, as illustrated in Figure 1, previous methods [1, 2] do not fully explore the geometry of the scene, particularly the occlusion caused by walls which affect sound propagation and can be extracted from input videos. In this work, we explicitly model the effects of room geometry and occlusions on spatial audio generation, enhancing the ability to model sound propagation in large scenes, especially those with multiple rooms and walls.

More specifically, the sound energy attenuates over distance and is reflected off or absorbed by surfaces as it propagates through space [10]. The sound energy received at a 3D position is determined by the full 3D scene geometry. Therefore, we first learn a NeRF [2] to provide the implicit 3D scene geometry. To better model the sound field, we derive a scene occlusion-aware prior, termed the global acoustic field, based on distance-aware parametric sound propagation modelling centred at the sound source and transformed by the learned transmittance from NeRF. We then extract the feature from the local acoustic field around the receiver using a Fibonacci Sphere, followed by a direction-aware attention mechanism to obtain features. These derived priors and features are used to generate binaural audio at novel views, demonstrating superior performance.

In summary, our contributions are as follows: (i) We adopt the transmittance reshaped global prior for sound energy, enabling us to explicitly model scene occlusion on audio generation. (ii) Our direction-aware attention mechanism effectively captures useful local features for binaural audio generation. Extensive experiments on synthetic and real datasets, such as SoundSpace and RWAVS, demonstrate the superior performance of our approach compared to existing methods.

2 Related Work

Neural Radiance Fields and Implicit Surface. NeRF [3] has emerged as a promising representation of scene appearance and has been widely used in novel view synthesis. Subsequent works [4–9] extend NeRF in various aspects, including faster training [4–6], faster inference [7, 8], and handling in-the-wild images [9]. However, these methods struggle to extract high-quality surfaces due to insufficient surface constraints during optimisation. To solve this issue, NeuS [11] and VolSDF [12] propose utilising the signed distance function (SDF) as an implicit surface representation and develop new volume rendering methods to train neural SDF fields. Some following works like MonoSDF [13] and NeuRIS [14], demonstrate the effectiveness of incorporating monocular depth priors [13] and normal priors [13, 14] as additional geometric cues for learning implicit surface representation of indoor scenes from sequences of scene images. In our work, we adopt neural SDF fields for visual data synthesis which provides high-quality scene geometry for our occlusion-aware audio novel view synthesis.

Acoustic Fields. The representation of spatial sound fields has been studied extensively. Previous methods have either directly approximated acoustic fields with handcrafted priors [15–17] or focused solely on modelling perceptual cues with a parametric representations [18–20]. However, these methods often rely on strong assumptions. In recent years, researchers have shifted towards learning sound fields directly from data using neural networks. For instance, NAF [1] is the first method to leverage implicit representation to learn a neural acoustic field of RIR via an MLP. Unlike previous methods [15–20] that capture scene acoustics with handcrafted parameterisations, implicit representation encodes the scene acoustics in a more generic manner, enabling application to arbitrary scenes. INRAS [21] extends NAF by learning disentangled features for the emitter, scene geometry, and listener with known room boundaries. It reuses scene-dependent features for arbitrary emitter-listener pairs to generate higher fidelity RIR. Although INRAS integrates the scene environment by calculating the relative positions of the emitter and listener to scene boundary points, it still struggles to fully model the effect of scene structure on sound propagation. In contrast, we propose to utilise the high-quality geometry obtained from the neural SDF fields and explore sound energy priors based on this geometry to enhance audio generation.

Audio-visual Learning. Several recent works [22–35] have explored learning acoustic information from multimodal data information for different tasks, including sound localisation [23, 26], audio-visual navigation [24, 25], visual-acoustic matching [28, 29], dereverberation [30, 31], and audio separation [34, 35]. For novel view acoustic synthesis, ViGAS [36] combines auditory and visual observation from one viewpoint to render the sound received at the target viewpoint, assuming the sound source in the environment is visible in the input image and limited to a few views for audio generation. NACF [37] integrates multiple acoustic contexts into audio scene representation and proposes a multi-scale energy decay criterion for supervising generated RIR. Few-shotRIR [38] introduces a transformer-based model to extract multimodal features from few-shot audio-visual observations and predicts RIR for the queried source-receiver pair with a decoder module. BEE [39] reconstructs audio from sparse audio-visual samples by integrating obtained visual feature volumes with audio clips through cross-attention and rendering sound with learned time-frequency transformations. AV-NeRF [2] synthesises novel view audio by leveraging visual features extracted from images rendered from the novel view. In contrast, our approach learns a neural SDF field from input videos to represent scene geometry and explicitly models the effect of scene structure on sound propagation for more realistic spatial audio generation.

3 Task Definition

The task of audio-visual scene synthesis aims to synthesise visual frames and binaural audios for an arbitrary receiver (camera and binaural microphone) trajectory within a static environment E . To synthesise new binaural audio a_t^* and generate a novel view image I^* , this task utilises observations $O = \{O_1, O_2, \dots, O_N\}$, where O_i consists of a receiver pose $\hat{\mathbf{p}}_{rc} = (\mathbf{p}_{rc}, \mathbf{d}_{rc})$ defined as the receiver position $\mathbf{p}_{rc} \in \mathbb{R}^3$ and direction $\mathbf{d}_{rc} \in \mathbb{R}^3$, a sound source position $\mathbf{p}_{sr} \in \mathbb{R}^3$, mono-source audio a_s , recorded binaural audio a_t , and an image I . The goal is to generate output binaural audio a_t^* and novel view image I^* from a new receiver pose $\hat{\mathbf{p}}_{rc}^*$ and source audio a_s^* . This process can be formulated as

$$(a_t^*, I^*) = f(\hat{\mathbf{p}}_{rc}^*, a_s^* | O, E), \quad (1)$$

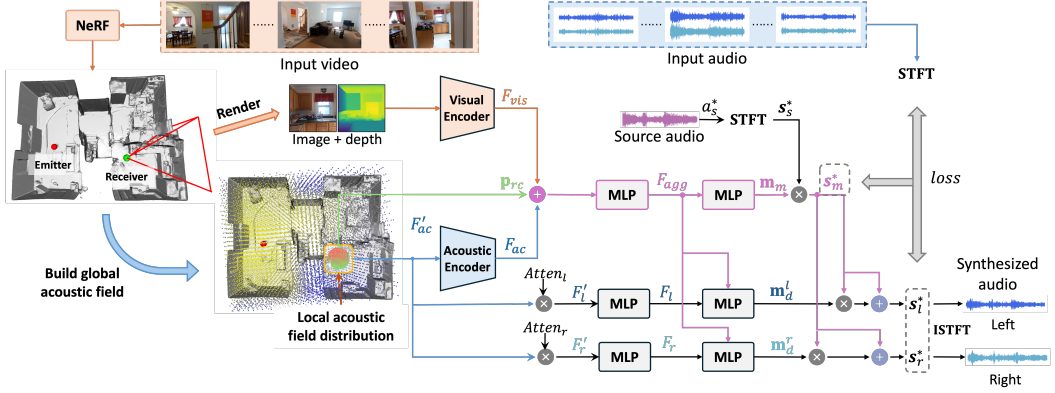


Figure 2: The pipeline of our proposed SOAF method. Starting with calibrated video, we reconstruct the scene using NeRF and build the global acoustic field. For novel view audio synthesis, the distribution of the local acoustic field F_{ac} , combined with visual features F_{vis} and the receiver's position p_{rc} , is fed into the network to predict the mixture acoustic mask m_m . The difference masks m_d^l and m_d^r are determined by the proposed direction-aware attention mechanism. Binaural sound is synthesised by fusing the magnitude of input audio and predicted masks m_m , m_d^l and m_d^r .

where f denotes the synthesis function. Similar to existing works [2], the position of the sound source is assumed to be known in the environment E . Literature commonly adopts two strategies to present the synthesis function, such as acoustic mask [2] and Room Impulse Response (RIR) [1, 21].

In this paper, our main focus lies not in network design but in introducing the *geometry prior* to the input. Our design can be applied to model both synthesis functions. In Section 4, we present our approach to predict the acoustic mask; an alternative version of predicting the room impulse response is provided in the supplementary material.

4 Method

We first introduce the acoustic-mask based audio synthesis function and provide an overview of our pipeline in Section 4.1. Then, we include novel view visual feature extraction in Section 4.2, details of our main contribution: global-local acoustic field generation in Section 4.3, and the direction-aware attention mechanism in Section 4.4. At last, we present the learning objective in Section 4.5.

4.1 Overview

Acoustic Mask. We adopt the acoustic mask-based synthesis function introduced in AV-NeRF [2] for binaural audio prediction. Specifically, the acoustic mask consists of $m_m, m_d^l, m_d^r \in \mathbb{R}^{F \times W}$, where F represents the frequency bins and W is the number of time frames. m_m captures changes in audio magnitude at the receiver position p_{rc} relative to the sound source position p_{sr} , m_d^l and m_d^r characterise the changes for left and right channels of the binaural audio. Given the Short-Time Fourier Transform (STFT) of the input audio clip a_s^* , defined as $s_s^* = \text{STFT}(a_s^*)$ and predicted acoustic masks m_m, m_d^l, m_d^r , we can synthesise the changed magnitude of the binaural audio as

$$s_m^* = s_s^* \odot m_m, \quad s_l^* = s_m^* + s_m^* \odot m_d^l, \quad s_r^* = s_m^* + s_m^* \odot m_d^r \quad (2)$$

where \odot denotes element-wise multiplication operation, s_l^* and s_r^* represent the magnitude of the synthesised left and right channel of the audio, respectively. Finally, we can obtain the binaural audio as $a_t^* = [\text{ISTFT}(s_l^*), \text{ISTFT}(s_r^*)]$ where ISTFT denotes the inverse STFT, s_l^* and s_r^* are for left and right channel, respectively.

An overview of our work is shown in Figure 2. Our framework consists of a NeRF for geometry and novel view synthesis to extract visual and local geometric features, then builds the global acoustic field and local acoustic field for obtaining the audio feature for masks prediction. We provide details below.

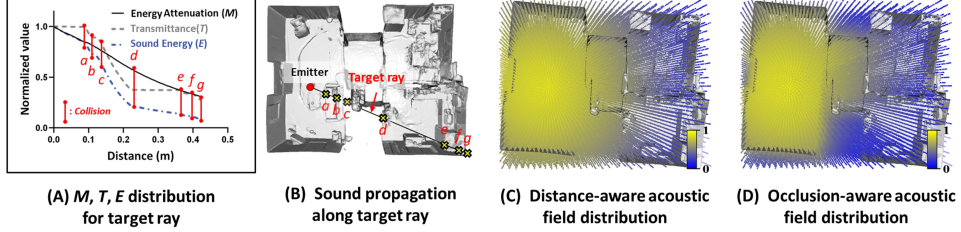


Figure 3: Illustration of global acoustic field generation. **(A)** The distribution of energy absorption M , acoustic transmittance T , and sound energy E for the target ray. Decreasing M correlates with increased propagation distance, and T varies with energy decay during sound wave collisions. E combines M and T . **(B)** Sound waves propagate through walls along the target ray, with collision marked by yellow crosses. **(C-D)** Distribution of distance-aware and occlusion-aware acoustic fields.

4.2 Novel-view Visual Feature Extraction

Similar to AV-NeRF [2], we learn a NeRF from the input image sequence. In particular, we adopt SDFStudio [40] which parameterised the radiance field by a signed distance function (SDF), enabling us to obtain scene geometry of better quality than AV-NeRF [2] and the occlusions in the scene. We can render a single image and depth map at the receiver location and the novel view, capturing the visual information of the novel view. We extract the feature F_{vis} from the rendered image and depth using a simple encoder locally which is then used for mask prediction.

4.3 Global and Local Acoustic Field

Global Acoustic Field describes sound waves radiating from a central sound source, considering (i) *distance-aware* energy attenuation and (ii) absorption by *occlusion*. To generate these waves, we place the sound source at the centre of a sphere and uniformly sample K points on the sphere’s surface using the Fibonacci Sphere sampling [41]. We then emit rays from the centre of the sphere through these points to obtain K rays. After that, we uniformly sample N points along each ray to have sampled points \mathbf{p}_i , where $i \in \{1, 2, \dots, N\}$. Each point \mathbf{p}_i corresponds to sound energy E_i at that location. We refer to the sound energy distribution of sampled points generated by the sound source as the global acoustic field.

Distance-aware. The sound energy at each sampled point along the ray decreases with increasing distance. The room acoustic rendering proposed by Siltanen *et al.* [42] analyses the time-dependent sound transport in a path tracing framework. It accounts for energy absorption and time delay due to propagation media and distance, introducing $M(\mathbf{p}_{rc}, \mathbf{p}_{sr}, t)$ to quantify energy attenuation. We define $d(\mathbf{p}_{rc}, \mathbf{p}_{sr}) = \|\mathbf{p}_{rc} - \mathbf{p}_{sr}\|_2$. The process can be defined as

$$M(\mathbf{p}_{rc}, \mathbf{p}_{sr}, t) = e^{-\sigma d(\mathbf{p}_{rc}, \mathbf{p}_{sr})} \delta\left(t - \frac{d(\mathbf{p}_{rc}, \mathbf{p}_{sr})}{c}\right), \quad (3)$$

where c is the speed of sound, σ is the absorption factor, and $\delta(t)$ is the Dirac delta function. We reformulated the equation by ignoring the time-delay component for now. The distance-aware part of sound energy absorption $M(\mathbf{p}_i, \mathbf{p}_{sr})$ at point \mathbf{p}_i can be written as

$$M(\mathbf{p}_i, \mathbf{p}_{sr}) = e^{-\sigma d(\mathbf{p}_i, \mathbf{p}_{sr})}. \quad (4)$$

Figure 3.A describes the variation of M with increasing distance between \mathbf{p}_i and \mathbf{p}_{sr} .

Occlusion-aware. In neural volume rendering [3], visual transmittance handles occlusion. When rendering the colour of the pixel from the sampled points along the ray, points closer to the camera with high density α contribute more to the colour than farther ones. Drawing on this principle, we adapt this technique to address occlusion in sound propagation. Despite the fundamental differences between sound, a mechanical wave that can penetrate obstacles and light, an electromagnetic wave that cannot, our approach innovates upon the established methodology to enhance sound propagation modelling.

Given the trained NeRF, it allows us to determine the density α_i of each point \mathbf{p}_i in the 3D space. In order to allow sound waves to penetrate obstacles, we propose acoustic transmittance T - we

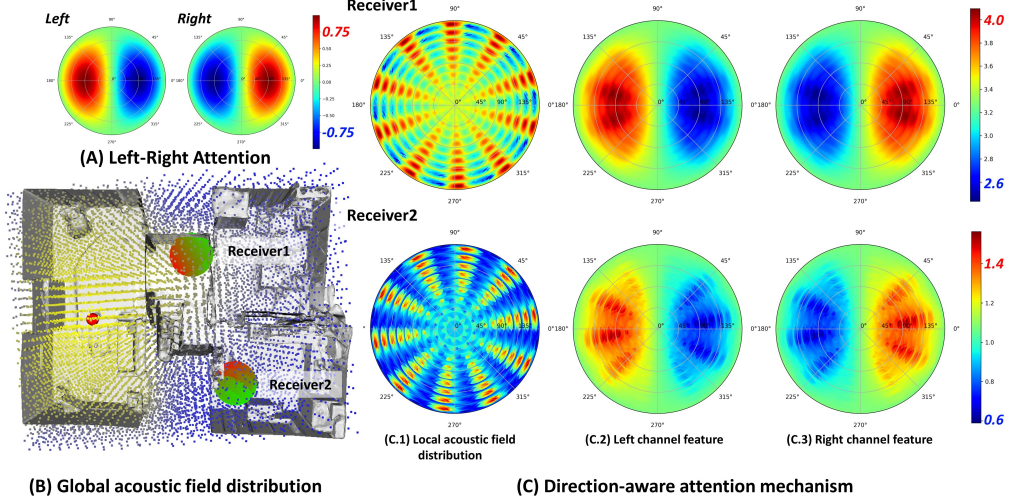


Figure 4: Binaural feature generated by direction-aware attention mechanism. **(A)** Predefined left-right attention. **(B)** Local distribution of two receivers: Receiver 1 in the hallway, close to the sound source with higher energy; Receiver 2 in the kitchen, further away and obstructed with lower energy. Energy comparison is highlighted in the sub-figure C colour bar. **(C)** Direction-aware attention mechanism: The binaural features describe the spatial and directional sound characteristics, generated by the combination of the left-right attention and the local acoustic field distribution.

multiply visual transmittance by the attenuation coefficient γ , which depends on the scene geometry. Combined with the distance-aware energy attenuation, the final sound energy E_i at each point \mathbf{p}_i can be defined as:

$$\alpha_i = \alpha_i \times \gamma, \quad T_i = \prod_{j=1}^i (1 - \alpha_j), \quad E_i = M(\mathbf{p}_i, \mathbf{p}_{sr}) \times T_i. \quad (5)$$

Figure 3.B depicts sound waves from a source traversing seven surfaces along a target ray. Figure 3.A quantitatively captures sound energy, accounting for both propagation distance and obstructions. Figure 3.CD demonstrates the efficacy of our method in managing occlusions in sound propagation.

Local Acoustic Field depicts the distribution of sound energy around the receiver. Inspired by the design of spherical microphone arrays [43], we generate a Fibonacci Sphere around the receiver to collect the sound energy in the global acoustic field. Specifically, a Fibonacci Sphere centre is the centre of the local coordinate system with G points on the surface. Rays are emitted from the centre, passing through the sphere's surface, in the direction $\mathbf{d}_{Fib} \in \mathbb{R}^{3 \times G}$. H points are uniformly sampled along these rays within the range r_{min} to r_{max} . The sampled points are then transformed from the local to the world coordinate system by the receiver's pose. We use the nearest interpolation to extract sound energy for each sampled point from the global acoustic field. The local acoustic field is a $G \times H$ feature vector (with G rays, each having H sampled points containing interpolated wave energy). We compute a distance-weighted sum of wave energy along each ray, resulting in $F'_{ac} \in \mathbb{R}^G$, which is then input into the acoustic encoder to obtain F_{ac} . As shown in Figure 2, combining the feature F_{ac} predicted from the local acoustic field, F_{vis} and feature of the receiver location \mathbf{p}_{rc} as F_{agg} , we can estimate the sound attenuation mask \mathbf{m}_m at the receiver location from F_{agg} .

4.4 Direction-aware Attention Mechanism

Given the Local Acoustic Field, we propose a direction-aware attention mechanism to distinguish the left and right channel sound features to generate the binaural audio. Specifically, we calculate the similarity between the left or right channel directions $\mathbf{d}_l, \mathbf{d}_r \in \mathbb{R}^3$ with \mathbf{d}_{Fib} to obtain the attention $Atten_l, Atten_r \in \mathbb{R}^G$ for each channel. This attention is then combined with the local acoustic field to obtain binaural features. The process can be defined as: $Atten_l = \mathbf{d}_l^T \mathbf{d}_{Fib}$, $F'_l = Atten_l^T \odot F'_{ac}$, $Atten_r = \mathbf{d}_r^T \mathbf{d}_{Fib}$, $F'_r = Atten_r^T \odot F'_{ac}$, where \odot denotes element-wise multiplication. After further transformation of F'_l and F'_r to F_l and F_r , respectively, to align their dimension with F_{agg} , we combine F_{agg} with F_l or F_r separately to estimate \mathbf{m}_d^l or \mathbf{m}_d^r . Figure 4

compares the local acoustic fields and binaural channel features for two receivers at different positions. The patterns of the two different receivers indicate their distinct directions, and the colour bar shows the differing sound intensities of their left and right channels. The directions and sound intensities of binaural channels are considered comprehensively in scene occlusion-aware sound propagation.

4.5 Learning Objective

Acoustic Mask. In the RWAVS dataset, we predict the \mathbf{m}_m and \mathbf{m}_d^l , \mathbf{m}_d^r and obtain the predicted magnitudes \mathbf{s}_m^* , \mathbf{s}_l^* , \mathbf{s}_r^* via Equation 2. Following the approach in [2], we optimise the network with the following loss function:

$$\mathcal{L}_A = \|\mathbf{s}_m - \mathbf{s}_m^*\|^2 + \|\mathbf{s}_l - \mathbf{s}_l^*\|^2 + \|\mathbf{s}_r - \mathbf{s}_r^*\|^2, \quad (6)$$

where \mathbf{s}_m , \mathbf{s}_l and \mathbf{s}_r denote the ground-truth magnitudes, corresponding to the mixture, left, and right channels, respectively. The mixture \mathbf{s}_m is defined as the average of \mathbf{s}_l and \mathbf{s}_r . The first term of \mathcal{L}_A encourages the network to predict the masks reflecting spatial effects caused by distance and geometry-occlusion. The second and third terms encourage the network to generate masks that capture differences between the binaural channels.

5 Experiments

5.1 Datasets, Baselines & Metrics

Datasets. We evaluate our method on the real-world RWAVS and the synthetic SoundSpaces datasets.

RWAVS dataset. The Real-World Audio-Visual Scene (RWAVS) dataset is collected by the authors of AV-NeRF [2] from diverse real-world scenarios, divided into four categories: *office*, *house*, *apartment*, and *outdoor* environments. Specifically, the indoor scenes have single-room layouts in the *office* category, while multi-room layouts are present in the *house* and *apartment* categories. To capture various acoustic and visual signals along different camera trajectories, the data collector moved randomly through the environment while holding the recording device. For each scene, RWAVS contains multimodal data including source audio, collected high-quality binaural audio, video, and camera poses, ranging from 10 to 25 minutes. Camera positions are densely distributed throughout the scene, and camera directions are sufficiently diverse. For a fair comparison, we maintain the same training/test split as [2], which contains 9,850 samples for training and 2,469 samples for testing, respectively.

SoundSpaces dataset. SoundSpaces [24, 44] is a synthetic dataset simulated based on hybrid sound propagation methods [45–47] that simulates fine-grained acoustic properties by simultaneously considering the effects of room geometry and surface materials on sound propagation in a 3D environment. Following the approach in [1, 21, 2], we validate our method on the same six representative indoor scenes, including two single rooms with rectangular walls, two single rooms with non-rectangular walls, and two multi-room layouts. For each scene, SoundSpaces provides binaural impulse responses for extensive emitter and receiver pairs sampled within the room at a fixed height from four different head orientations (0°, 90°, 180°, and 270°). To validate the effectiveness of our approach on this dataset, we modify our model to estimate binaural impulse responses instead of acoustic masks while keeping all other components unchanged. We keep the same training/test split as previous works [1, 21, 2] by using 90% data for training and 10% data for testing.

Baselines. We compare our approach with state-of-the-art methods [1, 21, 36, 2] that also learn a neural acoustic field with implicit representation. Among these methods, NAF [1] learns audio signals with a trainable local feature grid while INRAS [21] disentangles scene-dependent features from audio signals and reuses them for all emitter-listener pairs. ViGAS [36] and AV-NeRF [2] are multimodal approaches that leverage the visual feature of a single image for audio generation. For the RWAVS dataset, we include three additional baselines for reference: Mono-Mono, Mono-Energy, and Stereo-Energy. Mono-Mono simply repeats the source audio twice to achieve a binaural effect. Mono-Energy scales the energy of the source audio to match the average energy of the ground truth target audio then duplicates it to obtain a binaural audio. Stereo-Energy first duplicates the source audio and then scales the two channels separately to match the energy of each channel of the ground truth target audio. For the SoundSpaces dataset, we also compare our model with the linear and nearest neighbour interpolation results of two widely used audio coding methods: Advanced Audio

Methods	Office w/o occ		House w/ occ		Apartment w/ occ		Outdoors w/o occ		Overall	
			MAG↓	ENV↓	MAG↓	ENV↓	MAG↓	ENV↓	MAG↓	ENV↓
	MAG↓	ENV↓	MAG↓	ENV↓	MAG↓	ENV↓	MAG↓	ENV↓	MAG↓	ENV↓
Mono-Mono	9.269	0.411	11.889	0.424	15.120	0.474	13.957	0.470	12.559	0.445
Mono-Energy	1.536	0.142	4.307	0.180	3.911	0.192	1.634	0.127	2.847	0.160
Stereo-Energy	1.511	0.139	4.301	0.180	3.895	0.191	1.612	0.124	2.830	0.159
INRAS [21]	1.405	0.141	3.511	0.182	3.421	0.201	1.502	0.130	2.460	0.164
NAF [1]	1.244	0.137	3.259	0.178	3.345	0.193	1.284	0.121	2.283	0.157
ViGAS [36]	1.049	0.132	2.502	0.161	2.600	0.187	1.169	0.121	1.830	0.150
AV-NeRF [2]	0.930	0.129	2.009	0.155	2.230	0.184	0.845	0.111	1.504	0.145
SOAF	0.828	0.126	1.951	0.153	2.097	0.182	0.770	0.109	1.411	0.142

Table 1: Quantitative results on RWAVS dataset. Our method consistently outperforms all baselines in MAG and ENV metrics. “w/ occ” denotes a multi-room indoor scene with *occclusion*.

Methods	Large 1 w/ occ	Large 2 w/ occ	Medium 1 w/ occ	Medium 2 w/ occ	Small 1 w/o occ	Small 2 w/o occ	Mean							
	Spec↓ T60↓	Spec↓ T60↓	Spec↓ T60↓	Spec↓ T60↓	Spec↓ T60↓	Spec↓ T60↓	Spec↓ T60↓							
AAC-nearest	1.913	9.996	1.989	13.31	2.111	6.148	2.122	6.051	2.296	9.798	2.509	5.809	1.999	7.979
AAC-linear	1.904	8.847	1.964	11.63	2.105	4.585	2.116	4.422	2.299	8.253	2.521	6.021	1.998	7.208
Opus-nearest	1.740	12.20	1.817	15.15	1.887	7.875	1.898	7.897	2.058	10.68	2.238	7.564	1.907	9.493
Opus-linear	1.780	11.30	1.827	13.55	1.922	6.710	1.934	6.917	2.097	9.116	2.284	6.981	1.941	8.621
NAF [1]	0.396	4.166	0.413	6.075	0.384	3.110	0.384	3.072	0.356	3.378	0.344	2.098	0.380	3.650
INRAS [21]	0.391	4.113	0.408	5.998	0.379	3.070	0.380	3.033	0.351	3.335	0.339	2.071	0.375	3.604
AV-NeRF [2]	0.388	3.424	0.403	3.312	0.381	2.703	0.377	2.746	0.341	3.384	0.323	2.039	0.369	2.935
SOAF	0.380	2.319	0.394	2.627	0.373	2.144	0.369	2.099	0.334	2.763	0.317	2.014	0.361	2.327

Table 2: Quantitative results on Soundsapces dataset. Our method consistently outperforms all baselines in spectral loss (Spec) and T60 percentage error. “w/ occ” denotes an indoor scene with *occlusion*.

Coding (AAC) [48] and Xiph Opus [49]. All these methods are evaluated with the same train/test split for each dataset.

Metrics. Following AV-NeRF [2], we utilise the magnitude distance (MAG) [50] and envelope distance (ENV) [51] as evaluation metrics on the RWAVS dataset. MAG measures the audio quality of the generated sound in the time-frequency domain after applying the Short-Time Fourier Transform (STFT), while ENV measures it in the time domain. On the SoundSpaces dataset, we follow NAF [1] to evaluate our method with a) the spectral loss, which is the magnitude distance between the generated and the ground truth log-spectrogram, and b) the T60 error, which describes the percentage error between the time it takes for the synthesised RIR to decay by 60 dB in the time domain with the ground truth T60 reverberation time. For all of these metrics, lower is better. The detailed definitions of these metrics are provided in the supplementary materials.

5.2 Results & Ablation study

We present the quantitative experimental results on the RWAVS dataset in Table 1. Our model consistently outperforms all baselines across all environments. Specifically, we achieve an overall 6.2% and 22.9% reduction in the MAG metric compared to previous state-of-the-art audio-visual methods AV-NeRF [2] and ViGAS [36], respectively. This demonstrates that our approach can extract more comprehensive environmental information from visual inputs and efficiently integrate it into the neural acoustic field modelling. Table 2 provides the quantitative results on the Soundsapces dataset. Compared to all previous methods, our approach achieves the best performance in both spectral loss (Spec) and T60 percentage error for all scenes, especially for large indoor scenes with multi-room layouts. In particular, we obtain an overall 20.7% reduction in T60 error across all scenes, and an average 26.5% reduction on multi-room scenes *Large 1* and *Large 2*. This greater improvement in multi-room scenes further validates the effectiveness of our global-local acoustic field in modelling sound propagation in complex scene layouts with occlusions. An example of a visual comparison of

Methods	Office		House		Apartment		Outdoors		Overall	
	MAG↓	ENV↓								
Ours - w/o geo, dir	0.929	0.129	2.017	0.155	2.262	0.184	0.820	0.110	1.507	0.145
Ours - w/o dir	0.854	0.126	1.960	0.153	2.122	0.182	0.802	0.110	1.434	0.143
Ours - full	0.828	0.126	1.951	0.153	2.097	0.182	0.770	0.109	1.411	0.142

Table 3: Ablation study of proposed components on RWAVS dataset. “geo” is global-local acoustic field, “dir” is direction-aware attention mechanism and “full” denotes all proposed modules.

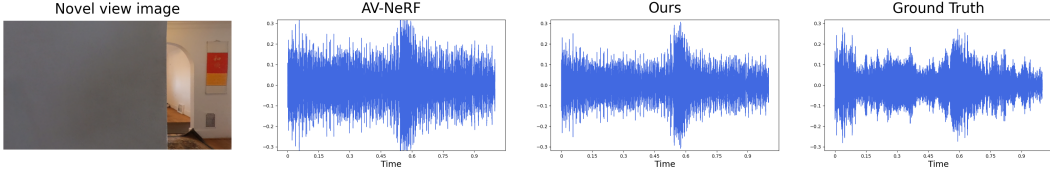


Figure 5: Example visual comparison of the synthesised audio (left channel) rendered from the novel view in the left image. Compared with AV-NeRF [2], our method attenuates more accurately the sound energy of the source audio, which is emitted from the right side of the receiver.

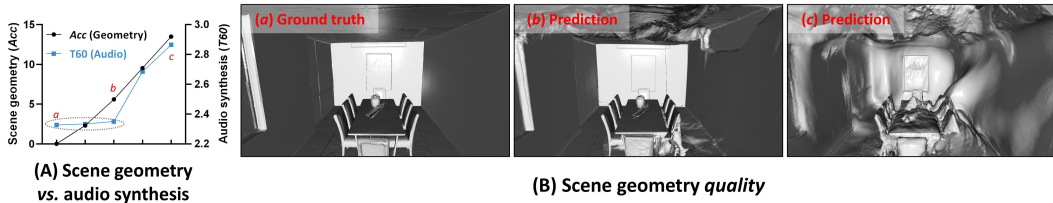


Figure 6: Robustness to scene reconstruction quality. **Left:** audio synthesis performance with various geometry reconstructions. Small Acc and $T60$ are better. **Right:** visual differences in scene reconstruction results. a , b , and c correspond to the different geometry quality shown on the left.

rendered audio is shown in Figure 5. More implementation details are in the supplementary materials. Please refer to the project page for visualization.

Ablation Study of Proposed Components. We conducted an ablation study based on AV-NeRF on the RWAVS dataset. In Table 3, “w/o geo, dir” uses AV-NeRF’s default input (visual features, sound source, receiver location, and their relative direction). “w/o dir” only adds our global-local acoustic field (geo), showing improvements in all scenarios, especially in occluded multi-room settings, demonstrating the effectiveness of our spatial geometric prior. “Ours - w/o dir” uses AV-NeRF’s relative direction information and geo, while “Ours - full” incorporates all proposed modules, achieving the best performance by considering both the relative direction and occlusions.

Robustness to Scene Reconstruction Quality. Figure 6 illustrates the impact of scene geometry on audio synthesis. Even with worsening reconstructions (Acc from 0.01 to 6.5), performance remains stable, indicating robustness to geometric errors. Yet, significant degradation (Acc from 6.5 to 14), as shown on the Figure 6.B.c, reveals that inaccuracies in fundamental structures like walls can affect wave propagation, with incorrect layouts resulting in a noisy acoustic field.

6 Discussion

Limitation and Future work. (i) This method still relies on knowing the sound source position. (ii) Our proposed method does not model sound reflection and reverberation. (iii) Exploring sound sources with specific directional attributes could be a focus for future research.

Societal impact. Realistic reconstructions of audio-visual scenes enhance immersive experience in AR/VR games, but it may encourage players to spend more time on games. In addition, the spatial audio generated by our method might be susceptible to misuse for undesirable spoofing events.

Conclusion. In this work, we introduced a global-local acoustic field that significantly enhances audio-visual scene synthesis by incorporating room geometry and occlusions into sound propagation modelling. The proposed direction-aware attention mechanism delivers more accurate and realistic binaural audio in complex environments. Tested on both the RWAWS and SoundSpaces datasets, our approach enhances immersive experiences in augmented and virtual reality applications and shows promise for further advancements across various settings.

References

- [1] Andrew Luo, Yilun Du, Michael Tarr, Josh Tenenbaum, Antonio Torralba, and Chuang Gan. Learning neural acoustic fields. *Advances in Neural Information Processing Systems*, 35: 3165–3177, 2022.
- [2] Susan Liang, Chao Huang, Yapeng Tian, Anurag Kumar, and Chenliang Xu. Av-nerf: Learning neural fields for real-world audio-visual scene synthesis. *Advances in Neural Information Processing Systems*, 36, 2024.
- [3] Ben Mildenhall, Pratul P Srinivasan, Matthew Tancik, Jonathan T Barron, Ravi Ramamoorthi, and Ren Ng. Nerf: Representing scenes as neural radiance fields for view synthesis. *Communications of the ACM*, 65(1):99–106, 2021.
- [4] Sara Fridovich-Keil, Alex Yu, Matthew Tancik, Qinhong Chen, Benjamin Recht, and Angjoo Kanazawa. Plenoxels: Radiance fields without neural networks. In *Proceedings of the IEEE/CVF Conference on Computer Vision and Pattern Recognition*, pages 5501–5510, 2022.
- [5] Anpei Chen, Zexiang Xu, Andreas Geiger, Jingyi Yu, and Hao Su. Tensorf: Tensorial radiance fields. In *European Conference on Computer Vision*, pages 333–350. Springer, 2022.
- [6] Thomas Müller, Alex Evans, Christoph Schied, and Alexander Keller. Instant neural graphics primitives with a multiresolution hash encoding. *ACM transactions on graphics (TOG)*, 41(4): 1–15, 2022.
- [7] Christian Reiser, Songyou Peng, Yiyi Liao, and Andreas Geiger. Kilonerf: Speeding up neural radiance fields with thousands of tiny mlps. In *Proceedings of the IEEE/CVF international conference on computer vision*, pages 14335–14345, 2021.
- [8] Alex Yu, Ruilong Li, Matthew Tancik, Hao Li, Ren Ng, and Angjoo Kanazawa. Plenotrees for real-time rendering of neural radiance fields. In *Proceedings of the IEEE/CVF International Conference on Computer Vision*, pages 5752–5761, 2021.
- [9] Ricardo Martin-Brualla, Noha Radwan, Mehdi SM Sajjadi, Jonathan T Barron, Alexey Dosovitskiy, and Daniel Duckworth. Nerf in the wild: Neural radiance fields for unconstrained photo collections. In *Proceedings of the IEEE/CVF Conference on Computer Vision and Pattern Recognition*, pages 7210–7219, 2021.
- [10] Steven L Garrett and Steven L Garrett. Attenuation of sound. *Understanding Acoustics: An Experimentalist’s View of Sound and Vibration*, pages 673–698, 2020.
- [11] Peng Wang, Lingjie Liu, Yuan Liu, Christian Theobalt, Taku Komura, and Wenping Wang. Neus: Learning neural implicit surfaces by volume rendering for multi-view reconstruction. *arXiv preprint arXiv:2106.10689*, 2021.
- [12] Lior Yariv, Jiatao Gu, Yoni Kasten, and Yaron Lipman. Volume rendering of neural implicit surfaces. *Advances in Neural Information Processing Systems*, 34:4805–4815, 2021.
- [13] Zehao Yu, Songyou Peng, Michael Niemeyer, Torsten Sattler, and Andreas Geiger. Monosdf: Exploring monocular geometric cues for neural implicit surface reconstruction. *Advances in neural information processing systems*, 35:25018–25032, 2022.
- [14] Jiepeng Wang, Peng Wang, Xiaoxiao Long, Christian Theobalt, Taku Komura, Lingjie Liu, and Wenping Wang. Neuris: Neural reconstruction of indoor scenes using normal priors. In *European Conference on Computer Vision*, pages 139–155. Springer, 2022.

[15] Rémi Mignot, Gilles Chardon, and Laurent Daudet. Low frequency interpolation of room impulse responses using compressed sensing. *IEEE/ACM Transactions on Audio, Speech, and Language Processing*, 22(1):205–216, 2013.

[16] Niccolo Antonello, Enzo De Sena, Marc Moonen, Patrick A Naylor, and Toon Van Waterschoot. Room impulse response interpolation using a sparse spatio-temporal representation of the sound field. *IEEE/ACM Transactions on Audio, Speech, and Language Processing*, 25(10):1929–1941, 2017.

[17] Natsuki Ueno, Shoichi Koyama, and Hiroshi Saruwatari. Kernel ridge regression with constraint of helmholtz equation for sound field interpolation. In *2018 16th International Workshop on Acoustic Signal Enhancement (IWAENC)*, pages 1–440. IEEE, 2018.

[18] Nikunj Raghuvanshi and John Snyder. Parametric wave field coding for precomputed sound propagation. *ACM Transactions on Graphics (TOG)*, 33(4):1–11, 2014.

[19] Nikunj Raghuvanshi and John Snyder. Parametric directional coding for precomputed sound propagation. *ACM Transactions on Graphics (TOG)*, 37(4):1–14, 2018.

[20] Chakravarty R Alla Chaitanya, Nikunj Raghuvanshi, Keith W Godin, Zechen Zhang, Derek Nowrouzezahrai, and John M Snyder. Directional sources and listeners in interactive sound propagation using reciprocal wave field coding. *ACM Transactions on Graphics (TOG)*, 39(4):44–1, 2020.

[21] Kun Su, Mingfei Chen, and Eli Shlizerman. Inras: Implicit neural representation for audio scenes. *Advances in Neural Information Processing Systems*, 35:8144–8158, 2022.

[22] Hang Zhao, Chuang Gan, Andrew Rouditchenko, Carl Vondrick, Josh McDermott, and Antonio Torralba. The sound of pixels. In *Proceedings of the European conference on computer vision (ECCV)*, pages 570–586, 2018.

[23] Yapeng Tian, Jing Shi, Bochen Li, Zhiyao Duan, and Chenliang Xu. Audio-visual event localization in unconstrained videos. In *Proceedings of the European conference on computer vision (ECCV)*, pages 247–263, 2018.

[24] Changan Chen, Unnat Jain, Carl Schissler, Sebastia Vicenc Amengual Gari, Ziad Al-Halah, Vamsi Krishna Ithapu, Philip Robinson, and Kristen Grauman. Soundspaces: Audio-visual navigation in 3d environments. In *Computer Vision–ECCV 2020: 16th European Conference, Glasgow, UK, August 23–28, 2020, Proceedings, Part VI 16*, pages 17–36. Springer, 2020.

[25] Changan Chen, Ziad Al-Halah, and Kristen Grauman. Semantic audio-visual navigation. In *Proceedings of the IEEE/CVF Conference on Computer Vision and Pattern Recognition*, pages 15516–15525, 2021.

[26] Shentong Mo and Pedro Morgado. Localizing visual sounds the easy way. In *European Conference on Computer Vision*, pages 218–234. Springer, 2022.

[27] Ruohan Gao and Kristen Grauman. 2.5 d visual sound. In *Proceedings of the IEEE/CVF Conference on Computer Vision and Pattern Recognition*, pages 324–333, 2019.

[28] Changan Chen, Ruohan Gao, Paul Calamia, and Kristen Grauman. Visual acoustic matching. In *Proceedings of the IEEE/CVF Conference on Computer Vision and Pattern Recognition*, pages 18858–18868, 2022.

[29] Arjun Somayazulu, Changan Chen, and Kristen Grauman. Self-supervised visual acoustic matching. *Advances in Neural Information Processing Systems*, 36, 2024.

[30] Changan Chen, Wei Sun, David Harwath, and Kristen Grauman. Learning audio-visual dereverberation. In *ICASSP 2023-2023 IEEE International Conference on Acoustics, Speech and Signal Processing (ICASSP)*, pages 1–5. IEEE, 2023.

[31] Sanjoy Chowdhury, Sreyan Ghosh, Subhrajyoti Dasgupta, Anton Ratnarajah, Utkarsh Tyagi, and Dinesh Manocha. Adverb: Visually guided audio dereverberation. In *Proceedings of the IEEE/CVF International Conference on Computer Vision*, pages 7884–7896, 2023.

[32] Yudong Guo, Keyu Chen, Sen Liang, Yong-Jin Liu, Hujun Bao, and Juyong Zhang. Ad-nerf: Audio driven neural radiance fields for talking head synthesis. In *Proceedings of the IEEE/CVF international conference on computer vision*, pages 5784–5794, 2021.

[33] Jinxing Zhou, Jianyuan Wang, Jiayi Zhang, Weixuan Sun, Jing Zhang, Stan Birchfield, Dan Guo, Lingpeng Kong, Meng Wang, and Yiran Zhong. Audio–visual segmentation. In *European Conference on Computer Vision*, pages 386–403. Springer, 2022.

[34] Hang Zhou, Xudong Xu, Dahua Lin, Xiaogang Wang, and Ziwei Liu. Sep-stereo: Visually guided stereophonic audio generation by associating source separation. In *Computer Vision–ECCV 2020: 16th European Conference, Glasgow, UK, August 23–28, 2020, Proceedings, Part XII 16*, pages 52–69. Springer, 2020.

[35] Yuxin Ye, Wenming Yang, and Yapeng Tian. Lavss: Location-guided audio-visual spatial audio separation. In *Proceedings of the IEEE/CVF Winter Conference on Applications of Computer Vision*, pages 5508–5519, 2024.

[36] Changan Chen, Alexander Richard, Roman Shapovalov, Vamsi Krishna Ithapu, Natalia Neverova, Kristen Grauman, and Andrea Vedaldi. Novel-view acoustic synthesis. In *Proceedings of the IEEE/CVF Conference on Computer Vision and Pattern Recognition*, pages 6409–6419, 2023.

[37] Susan Liang, Chao Huang, Yapeng Tian, Anurag Kumar, and Chenliang Xu. Neural acoustic context field: Rendering realistic room impulse response with neural fields. *arXiv preprint arXiv:2309.15977*, 2023.

[38] Sagnik Majumder, Changan Chen, Ziad Al-Halah, and Kristen Grauman. Few-shot audio-visual learning of environment acoustics. *Advances in Neural Information Processing Systems*, 35: 2522–2536, 2022.

[39] Mingfei Chen, Kun Su, and Eli Shlizerman. Be everywhere-hear everything (bee): Audio scene reconstruction by sparse audio-visual samples. In *Proceedings of the IEEE/CVF International Conference on Computer Vision*, pages 7853–7862, 2023.

[40] Zehao Yu, Anpei Chen, Bozidar Antic, Songyou Peng, Apratim Bhattacharyya, Michael Niemeyer, Siyu Tang, Torsten Sattler, and Andreas Geiger. Sdfstudio: A unified framework for surface reconstruction, 2022. URL <https://github.com/autonomousvision/sdfstudio>.

[41] Edward B Saff and Amo BJ Kuijlaars. Distributing many points on a sphere. *The mathematical intelligencer*, 19:5–11, 1997.

[42] Samuel Siltanen, Tapio Lokki, Sami Kiminki, and Lauri Savioja. The room acoustic rendering equation. *The Journal of the Acoustical Society of America*, 122(3):1624–1635, 2007.

[43] Boaz Rafaely. Analysis and design of spherical microphone arrays. *IEEE Transactions on speech and audio processing*, 13(1):135–143, 2004.

[44] Julian Straub, Thomas Whelan, Lingni Ma, Yufan Chen, Erik Wijmans, Simon Green, Jakob J Engel, Raul Mur-Artal, Carl Ren, Shobhit Verma, et al. The replica dataset: A digital replica of indoor spaces. *arXiv preprint arXiv:1906.05797*, 2019.

[45] Chunxiao Cao, Zhong Ren, Carl Schissler, Dinesh Manocha, and Kun Zhou. Interactive sound propagation with bidirectional path tracing. *ACM Transactions on Graphics (TOG)*, 35(6):1–11, 2016.

[46] Eric Veach and Leonidas Guibas. Bidirectional estimators for light transport. In *Photorealistic Rendering Techniques*, pages 145–167. Springer, 1995.

[47] M David Egan, JD Quirt, and MZ Rousseau. Architectural acoustics, 1989.

[48] International Organization for Standardization. Advanced audio coding (aac). *ISO/IEC 13818-7:2006*, 2006.

[49] Xiph.Org Foundation. Xiph opus. <https://opus-codec.org/>, 2012.

- [50] Xudong Xu, Hang Zhou, Ziwei Liu, Bo Dai, Xiaogang Wang, and Dahua Lin. Visually informed binaural audio generation without binaural audios. In *Proceedings of the IEEE/CVF Conference on Computer Vision and Pattern Recognition*, pages 15485–15494, 2021.
- [51] Pedro Morgado, Nuno Nvasconcelos, Timothy Langlois, and Oliver Wang. Self-supervised generation of spatial audio for 360 video. *Advances in neural information processing systems*, 31, 2018.
- [52] Changan Chen, Carl Schissler, Sanchit Garg, Philip Kobernik, Alexander Clegg, Paul Calamia, Dhruv Batra, Philip W Robinson, and Kristen Grauman. Soundspace 2.0: A simulation platform for visual-acoustic learning. In *NeurIPS 2022 Datasets and Benchmarks Track*, 2022.
- [53] Ziyang Chen, Israel D. Gebru, Christian Richardt, Anurag Kumar, William Laney, Andrew Owens, and Alexander Richard. Real acoustic fields: An audio-visual room acoustics dataset and benchmark. 2024.
- [54] Adam Paszke, Sam Gross, Francisco Massa, Adam Lerer, James Bradbury, Gregory Chanan, Trevor Killeen, Zeming Lin, Natalia Gimelshein, Luca Antiga, et al. Pytorch: An imperative style, high-performance deep learning library. *Advances in neural information processing systems*, 32, 2019.
- [55] P Kingma Diederik. Adam: A method for stochastic optimization. (*No Title*), 2014.
- [56] Julius O Smith. *Mathematics of the discrete Fourier transform (DFT): with audio applications*. Julius Smith, 2008.

A Predict Room Impulse Response and Learning Objective

Given an accurate model of the impulse-response for the left and right channel, $\text{rir}_l(\mathbf{p}_{sr}, \mathbf{p}_{rc}^*)$ and $\text{rir}_r(\mathbf{p}_{sr}, \mathbf{p}_{rc}^*)$, we may model audio reverberation of a_s emitted at \mathbf{p}_{sr} by computing the response, namely, the binaural audio, (a_{tl}, a_{tr}) , at the receiver location \mathbf{p}_{rc}^* by querying the continuous field and using temporal convolution:

$$a_{tl}^* = a_s \otimes \text{rir}_l(\mathbf{p}_{sr}, \mathbf{p}_{rc}^*), \quad a_{tr}^* = a_s \otimes \text{rir}_r(\mathbf{p}_{sr}, \mathbf{p}_{rc}^*) \quad (7)$$

The synthesis dataset Soundspace [24, 52], along with concurrent real-world dataset [53] are proposed to collect the Room Impulse Response for the scene.

Learning Objective. In the SoundSpace dataset, we predict Room Impulse Response across spectrogram time and frequency coordinates. We optimize the network via the spectral loss:

$$\mathcal{L}_R = \text{Spec}(\mathbf{m}_{\text{prd}}, \mathbf{m}_{\text{gt}}) \quad (8)$$

$$\mathbf{m}_{\text{gt}} = \text{STFT}(\text{rir}(\mathbf{p}_{sr}, \mathbf{p}_{rc}^*)), \quad \mathbf{m}_{\text{prd}} = \text{STFT}(\hat{\text{rir}}(\mathbf{p}_{sr}, \mathbf{p}_{rc}^*)), \quad (9)$$

where $\text{Spec}(\mathbf{m}_{\text{prd}}, \mathbf{m}_{\text{gt}})$ is the spectral loss function 12, $\text{rir}(\mathbf{p}_{sr}, \mathbf{p}_{rc}^*)$ is the ground truth RIR, $\hat{\text{rir}}(\mathbf{p}_{sr}, \mathbf{p}_{rc}^*)$ is the predicted RIR and $\mathbf{p}_{sr}, \mathbf{p}_{rc}^*$ are sound source position and synthesized receiver position respectively.

B Implementation Details

Our model is implemented using PyTorch [54] and optimized using the Adam [55] optimizer, with hyperparameters $\beta_1 = 0.9$ and $\beta_2 = 0.999$. The initial learning rate is set to 5×10^{-4} and is exponentially decreased to 5×10^{-6} . The training process spans 200 epochs, with a batch size of 32. In the RWAVS dataset, the absorption factor is $\sigma = 2.5$ and the attenuation coefficient is $\gamma = 0.01$. In the SoundSpace dataset, these values are $\sigma = 0.166$ and $\gamma = 0.66$. When building the Fibonacci Sphere, we set $G = 1024$ (uniformly generating 1024 rays around the sphere center) and $H = 10$ (uniformly sampling 10 points along each ray). In the RWAVS dataset, $r_{\min} = 0.001$ and $r_{\max} = 0.03$ and in the SoundSpace dataset, $r_{\min} = 0.1$ and $r_{\max} = 0.8$. The parameters, including the absorption factor σ , attenuation coefficient γ , and the characteristics of the Fibonacci Sphere, are determined based on the range and specific features of the scene. All experiments are conducted on an RTX 4090 GPU. For the RWAVS dataset, each scene is trained for 20 minutes, whereas for the SoundSpace dataset, each scene is trained for 25 hours.

C Evaluation Metrics

RWAVS dataset. We follow AV-NeRF [2] to select the magnitude distance (MAG) [50] and envelope distance (ENV) [51] as evaluation metrics on the RWAVS dataset.

The MAG metric is defined as

$$\text{MAG}(\mathbf{m}_{\text{prd}}, \mathbf{m}_{\text{gt}}) = \|\mathbf{m}_{\text{prd}} - \mathbf{m}_{\text{gt}}\|^2, \quad (10)$$

where \mathbf{m}_{prd} and \mathbf{m}_{gt} are the predicted and ground truth magnitude after applying the Short-Time Fourier Transform (STFT), respectively.

The ENV metric is defined as

$$\text{ENV}(a_{\text{prd}}, a_{\text{gt}}) = \|\text{hilbert}(a_{\text{prd}}) - \text{hilbert}(a_{\text{gt}})\|^2, \quad (11)$$

where a_{prd} is the predicted audio, a_{gt} is the ground truth audio, and hilbert is the Hilbert transformation function [56].

SoundSpaces dataset. We follow NAF [1] to use the spectral loss and T60 percentage error as evaluation metrics on the SoundSpaces dataset.

The spectral loss measures the log-magnitude distance by

$$\text{Spec}(\mathbf{m}_{\text{prd}}, \mathbf{m}_{\text{gt}}) = |\log(\mathbf{m}_{\text{prd}}) - \log(\mathbf{m}_{\text{gt}})|, \quad (12)$$

where \mathbf{m}_{prd} and \mathbf{m}_{gt} are the predicted and ground truth magnitude after applying STFT, respectively.

The T60 reverberation time is the time it takes for a sound to decay by 60 dB. We calculate the T60 percentage error by

$$T60(a_{\text{prd}}, a_{\text{gt}}) = \frac{|T60(a_{\text{prd}}) - T60(a_{\text{gt}})|}{T60(a_{\text{gt}})} , \quad (13)$$

where a_{prd} is the predicted impulse response and a_{gt} is the ground truth impulse response.

NeurIPS Paper Checklist

1. Claims

Question: Do the main claims made in the abstract and introduction accurately reflect the paper's contributions and scope?

Answer: [\[Yes\]](#)

Justification: Yes, we accurately claim our paper's contributions and scope in the abstract and introduction section. These claims are demonstrated in our methodology and experiments sections.

Guidelines:

- The answer NA means that the abstract and introduction do not include the claims made in the paper.
- The abstract and/or introduction should clearly state the claims made, including the contributions made in the paper and important assumptions and limitations. A No or NA answer to this question will not be perceived well by the reviewers.
- The claims made should match theoretical and experimental results, and reflect how much the results can be expected to generalize to other settings.
- It is fine to include aspirational goals as motivation as long as it is clear that these goals are not attained by the paper.

2. Limitations

Question: Does the paper discuss the limitations of the work performed by the authors?

Answer: [\[Yes\]](#)

Justification: We introduce the limitations of this work in the discussion section.

Guidelines:

- The answer NA means that the paper has no limitation while the answer No means that the paper has limitations, but those are not discussed in the paper.
- The authors are encouraged to create a separate "Limitations" section in their paper.
- The paper should point out any strong assumptions and how robust the results are to violations of these assumptions (e.g., independence assumptions, noiseless settings, model well-specification, asymptotic approximations only holding locally). The authors should reflect on how these assumptions might be violated in practice and what the implications would be.
- The authors should reflect on the scope of the claims made, e.g., if the approach was only tested on a few datasets or with a few runs. In general, empirical results often depend on implicit assumptions, which should be articulated.
- The authors should reflect on the factors that influence the performance of the approach. For example, a facial recognition algorithm may perform poorly when image resolution is low or images are taken in low lighting. Or a speech-to-text system might not be used reliably to provide closed captions for online lectures because it fails to handle technical jargon.
- The authors should discuss the computational efficiency of the proposed algorithms and how they scale with dataset size.
- If applicable, the authors should discuss possible limitations of their approach to address problems of privacy and fairness.
- While the authors might fear that complete honesty about limitations might be used by reviewers as grounds for rejection, a worse outcome might be that reviewers discover limitations that aren't acknowledged in the paper. The authors should use their best judgment and recognize that individual actions in favor of transparency play an important role in developing norms that preserve the integrity of the community. Reviewers will be specifically instructed to not penalize honesty concerning limitations.

3. Theory Assumptions and Proofs

Question: For each theoretical result, does the paper provide the full set of assumptions and a complete (and correct) proof?

Answer: [NA]

Justification: This paper does not include theoretical results and only includes experimental results.

Guidelines:

- The answer NA means that the paper does not include theoretical results.
- All the theorems, formulas, and proofs in the paper should be numbered and cross-referenced.
- All assumptions should be clearly stated or referenced in the statement of any theorems.
- The proofs can either appear in the main paper or the supplemental material, but if they appear in the supplemental material, the authors are encouraged to provide a short proof sketch to provide intuition.
- Inversely, any informal proof provided in the core of the paper should be complemented by formal proofs provided in appendix or supplemental material.
- Theorems and Lemmas that the proof relies upon should be properly referenced.

4. Experimental Result Reproducibility

Question: Does the paper fully disclose all the information needed to reproduce the main experimental results of the paper to the extent that it affects the main claims and/or conclusions of the paper (regardless of whether the code and data are provided or not)?

Answer: [Yes]

Justification: We include all the information needed to reproduce the main experimental results in the method section, experiment section, and supplementary material.

Guidelines:

- The answer NA means that the paper does not include experiments.
- If the paper includes experiments, a No answer to this question will not be perceived well by the reviewers: Making the paper reproducible is important, regardless of whether the code and data are provided or not.
- If the contribution is a dataset and/or model, the authors should describe the steps taken to make their results reproducible or verifiable.
- Depending on the contribution, reproducibility can be accomplished in various ways. For example, if the contribution is a novel architecture, describing the architecture fully might suffice, or if the contribution is a specific model and empirical evaluation, it may be necessary to either make it possible for others to replicate the model with the same dataset, or provide access to the model. In general, releasing code and data is often one good way to accomplish this, but reproducibility can also be provided via detailed instructions for how to replicate the results, access to a hosted model (e.g., in the case of a large language model), releasing of a model checkpoint, or other means that are appropriate to the research performed.
- While NeurIPS does not require releasing code, the conference does require all submissions to provide some reasonable avenue for reproducibility, which may depend on the nature of the contribution. For example
 - (a) If the contribution is primarily a new algorithm, the paper should make it clear how to reproduce that algorithm.
 - (b) If the contribution is primarily a new model architecture, the paper should describe the architecture clearly and fully.
 - (c) If the contribution is a new model (e.g., a large language model), then there should either be a way to access this model for reproducing the results or a way to reproduce the model (e.g., with an open-source dataset or instructions for how to construct the dataset).
 - (d) We recognize that reproducibility may be tricky in some cases, in which case authors are welcome to describe the particular way they provide for reproducibility. In the case of closed-source models, it may be that access to the model is limited in some way (e.g., to registered users), but it should be possible for other researchers to have some path to reproducing or verifying the results.

5. Open access to data and code

Question: Does the paper provide open access to the data and code, with sufficient instructions to faithfully reproduce the main experimental results, as described in supplemental material?

Answer: **[No]**

Justification: We will release all data and code after the paper is accepted.

Guidelines:

- The answer NA means that paper does not include experiments requiring code.
- Please see the NeurIPS code and data submission guidelines (<https://nips.cc/public/guides/CodeSubmissionPolicy>) for more details.
- While we encourage the release of code and data, we understand that this might not be possible, so “No” is an acceptable answer. Papers cannot be rejected simply for not including code, unless this is central to the contribution (e.g., for a new open-source benchmark).
- The instructions should contain the exact command and environment needed to run to reproduce the results. See the NeurIPS code and data submission guidelines (<https://nips.cc/public/guides/CodeSubmissionPolicy>) for more details.
- The authors should provide instructions on data access and preparation, including how to access the raw data, preprocessed data, intermediate data, and generated data, etc.
- The authors should provide scripts to reproduce all experimental results for the new proposed method and baselines. If only a subset of experiments are reproducible, they should state which ones are omitted from the script and why.
- At submission time, to preserve anonymity, the authors should release anonymized versions (if applicable).
- Providing as much information as possible in supplemental material (appended to the paper) is recommended, but including URLs to data and code is permitted.

6. Experimental Setting/Details

Question: Does the paper specify all the training and test details (e.g., data splits, hyper-parameters, how they were chosen, type of optimizer, etc.) necessary to understand the results?

Answer: **[Yes]**

Justification: We include the experimental details in the main paper and the supplementary material.

Guidelines:

- The answer NA means that the paper does not include experiments.
- The experimental setting should be presented in the core of the paper to a level of detail that is necessary to appreciate the results and make sense of them.
- The full details can be provided either with the code, in appendix, or as supplemental material.

7. Experiment Statistical Significance

Question: Does the paper report error bars suitably and correctly defined or other appropriate information about the statistical significance of the experiments?

Answer: **[No]**

Justification: This paper does not report error bars.

Guidelines:

- The answer NA means that the paper does not include experiments.
- The authors should answer “Yes” if the results are accompanied by error bars, confidence intervals, or statistical significance tests, at least for the experiments that support the main claims of the paper.
- The factors of variability that the error bars are capturing should be clearly stated (for example, train/test split, initialization, random drawing of some parameter, or overall run with given experimental conditions).

- The method for calculating the error bars should be explained (closed form formula, call to a library function, bootstrap, etc.)
- The assumptions made should be given (e.g., Normally distributed errors).
- It should be clear whether the error bar is the standard deviation or the standard error of the mean.
- It is OK to report 1-sigma error bars, but one should state it. The authors should preferably report a 2-sigma error bar than state that they have a 96% CI, if the hypothesis of Normality of errors is not verified.
- For asymmetric distributions, the authors should be careful not to show in tables or figures symmetric error bars that would yield results that are out of range (e.g. negative error rates).
- If error bars are reported in tables or plots, The authors should explain in the text how they were calculated and reference the corresponding figures or tables in the text.

8. Experiments Compute Resources

Question: For each experiment, does the paper provide sufficient information on the computer resources (type of compute workers, memory, time of execution) needed to reproduce the experiments?

Answer: **[Yes]**

Justification: We include the computer resources used for this work in the supplementary material.

Guidelines:

- The answer NA means that the paper does not include experiments.
- The paper should indicate the type of compute workers CPU or GPU, internal cluster, or cloud provider, including relevant memory and storage.
- The paper should provide the amount of compute required for each of the individual experimental runs as well as estimate the total compute.
- The paper should disclose whether the full research project required more compute than the experiments reported in the paper (e.g., preliminary or failed experiments that didn't make it into the paper).

9. Code Of Ethics

Question: Does the research conducted in the paper conform, in every respect, with the NeurIPS Code of Ethics <https://neurips.cc/public/EthicsGuidelines>?

Answer: **[Yes]**

Justification: This work conforms with the NeurIPS Code of Ethics.

Guidelines:

- The answer NA means that the authors have not reviewed the NeurIPS Code of Ethics.
- If the authors answer No, they should explain the special circumstances that require a deviation from the Code of Ethics.
- The authors should make sure to preserve anonymity (e.g., if there is a special consideration due to laws or regulations in their jurisdiction).

10. Broader Impacts

Question: Does the paper discuss both potential positive societal impacts and negative societal impacts of the work performed?

Answer: **[Yes]**

Justification: We present the potential positive and negative societal impacts in the discussion section.

Guidelines:

- The answer NA means that there is no societal impact of the work performed.
- If the authors answer NA or No, they should explain why their work has no societal impact or why the paper does not address societal impact.

- Examples of negative societal impacts include potential malicious or unintended uses (e.g., disinformation, generating fake profiles, surveillance), fairness considerations (e.g., deployment of technologies that could make decisions that unfairly impact specific groups), privacy considerations, and security considerations.
- The conference expects that many papers will be foundational research and not tied to particular applications, let alone deployments. However, if there is a direct path to any negative applications, the authors should point it out. For example, it is legitimate to point out that an improvement in the quality of generative models could be used to generate deepfakes for disinformation. On the other hand, it is not needed to point out that a generic algorithm for optimizing neural networks could enable people to train models that generate Deepfakes faster.
- The authors should consider possible harms that could arise when the technology is being used as intended and functioning correctly, harms that could arise when the technology is being used as intended but gives incorrect results, and harms following from (intentional or unintentional) misuse of the technology.
- If there are negative societal impacts, the authors could also discuss possible mitigation strategies (e.g., gated release of models, providing defenses in addition to attacks, mechanisms for monitoring misuse, mechanisms to monitor how a system learns from feedback over time, improving the efficiency and accessibility of ML).

11. Safeguards

Question: Does the paper describe safeguards that have been put in place for responsible release of data or models that have a high risk for misuse (e.g., pretrained language models, image generators, or scraped datasets)?

Answer: [NA]

Justification: This paper does not have a high risk for misuse.

Guidelines:

- The answer NA means that the paper poses no such risks.
- Released models that have a high risk for misuse or dual-use should be released with necessary safeguards to allow for controlled use of the model, for example by requiring that users adhere to usage guidelines or restrictions to access the model or implementing safety filters.
- Datasets that have been scraped from the Internet could pose safety risks. The authors should describe how they avoided releasing unsafe images.
- We recognize that providing effective safeguards is challenging, and many papers do not require this, but we encourage authors to take this into account and make a best faith effort.

12. Licenses for existing assets

Question: Are the creators or original owners of assets (e.g., code, data, models), used in the paper, properly credited and are the license and terms of use explicitly mentioned and properly respected?

Answer: [Yes]

Justification: We have cited the original owners of all assets that used in this paper properly.

Guidelines:

- The answer NA means that the paper does not use existing assets.
- The authors should cite the original paper that produced the code package or dataset.
- The authors should state which version of the asset is used and, if possible, include a URL.
- The name of the license (e.g., CC-BY 4.0) should be included for each asset.
- For scraped data from a particular source (e.g., website), the copyright and terms of service of that source should be provided.
- If assets are released, the license, copyright information, and terms of use in the package should be provided. For popular datasets, paperswithcode.com/datasets has curated licenses for some datasets. Their licensing guide can help determine the license of a dataset.

- For existing datasets that are re-packaged, both the original license and the license of the derived asset (if it has changed) should be provided.
- If this information is not available online, the authors are encouraged to reach out to the asset's creators.

13. New Assets

Question: Are new assets introduced in the paper well documented and is the documentation provided alongside the assets?

Answer: [NA]

Justification: This paper does not release new assets.

Guidelines:

- The answer NA means that the paper does not release new assets.
- Researchers should communicate the details of the dataset/code/model as part of their submissions via structured templates. This includes details about training, license, limitations, etc.
- The paper should discuss whether and how consent was obtained from people whose asset is used.
- At submission time, remember to anonymize your assets (if applicable). You can either create an anonymized URL or include an anonymized zip file.

14. Crowdsourcing and Research with Human Subjects

Question: For crowdsourcing experiments and research with human subjects, does the paper include the full text of instructions given to participants and screenshots, if applicable, as well as details about compensation (if any)?

Answer: [NA]

Justification: This paper does not involve crowdsourcing and human subjects.

Guidelines:

- The answer NA means that the paper does not involve crowdsourcing nor research with human subjects.
- Including this information in the supplemental material is fine, but if the main contribution of the paper involves human subjects, then as much detail as possible should be included in the main paper.
- According to the NeurIPS Code of Ethics, workers involved in data collection, curation, or other labor should be paid at least the minimum wage in the country of the data collector.

15. Institutional Review Board (IRB) Approvals or Equivalent for Research with Human Subjects

Question: Does the paper describe potential risks incurred by study participants, whether such risks were disclosed to the subjects, and whether Institutional Review Board (IRB) approvals (or an equivalent approval/review based on the requirements of your country or institution) were obtained?

Answer: [NA]

Justification: This paper does not involve crowdsourcing and human subjects.

Guidelines:

- The answer NA means that the paper does not involve crowdsourcing nor research with human subjects.
- Depending on the country in which research is conducted, IRB approval (or equivalent) may be required for any human subjects research. If you obtained IRB approval, you should clearly state this in the paper.
- We recognize that the procedures for this may vary significantly between institutions and locations, and we expect authors to adhere to the NeurIPS Code of Ethics and the guidelines for their institution.
- For initial submissions, do not include any information that would break anonymity (if applicable), such as the institution conducting the review.